Magnetic resonance force microscopy using ferromagnetic resonance of a magnetic tip excited by microwave transmission via a coaxial resonator

Yukinori Kinoshita[1] ⓘ**, Yan Jun Li**[2]**, Satoru Yoshimura**[1]**, Hitoshi Saito**[1] **and Yasuhiro Sugawara**[2]

[1] Research Center for Engineering Science, Graduate School of Engineering Science, Akita University, 1-1 Tegatagakuen-machi, Akita 010-8502, Japan
[2] Department of Applied Physics, Graduate School of Engineering, Osaka University, 2-1 Yamada-oka, Suita, Osaka 565-0871, Japan

E-mail: sugawara@ap.eng.osaka-u.ac.jp

CrossMark

Abstract

The present work proposes magnetic resonance force microscopy (MRFM) based on ferromagnetic resonance (FMR) modulation of a magnetic tip using microwave transmission via a coaxial resonator instead of using conventional microwave irradiation by an external antenna. In this MRFM, the coaxial resonator is electrically connected to the magnetic cantilever tip, which enables simple implementation of FMR excitation of a magnetic tip in conventional magnetic force microscopy. The FMR frequency of the tip can be easily extracted from the reflection spectrum of a transmission line connected to the magnetic tip. The excitation of tip FMR is confirmed from the microwave frequency dependence of the mechanical response of the tip oscillation. This MRFM is effective for extracting the magnetic interaction force near a sample surface without perturbation of its magnetic state. Nanometer-scale imaging of magnetic domain structures on a demagnetized thin-film permanent magnet is successfully demonstrated.
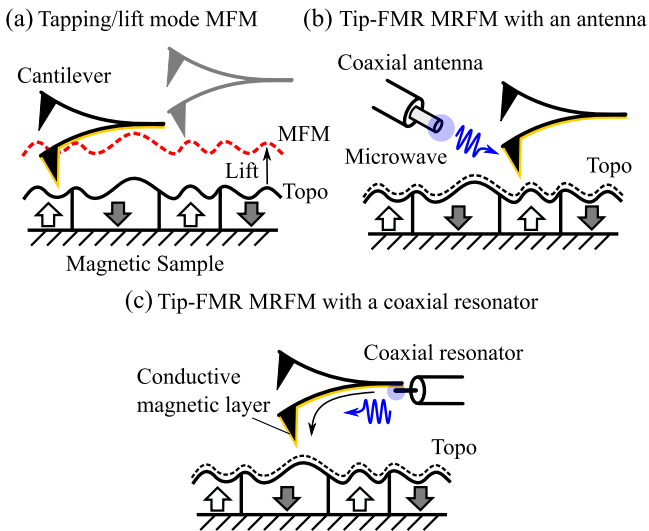
(Some figures may appear in colour only in the online journal)

1. Introduction

Since its invention, magnetic force microscope (MFM) [1, 2], has been widely used for evaluating the characteristics of magnetic materials and devices [3]. MFMs are capable of clarifying surface magnetic domain structures with high spatial resolution ($\sim$10 nm) noninvasively and without any environmental limitations. In a typical MFM, a magnetic cantilever tip is oscillated at a fixed frequency close to resonance and shifts of amplitude or phase of the cantilever oscillation, which are induced by tip-sample magnetic force, can be detected as MFM signals. Topographic signals are derived from a combination of short-ranged, strong, repulsive and long-ranged, weak, attractive (van der Waals) forces. To roughly separate the topographic signals from the long-ranged magnetic signals, differences in the tip-sample distance dependencies are used. This is accomplished by a tapping/lift mode [4] based on a two-pass scanning technique. In the tapping/lift mode, a topographic line is obtained in the tapping mode, and the tip is lifted and scanned once more over the measured topographic line with an offset distance while the MFM signals are detected (figure 1(a)).

Detection of MFM signals close to the surface is highly effective for resolving fine magnetic structures [5]. Typically,

(a) Tapping/lift mode MFM

Cantilever

MFM

Lift ↑ Topo

Magnetic Sample

(b) Tip-FMR MRFM with an antenna

Coaxial antenna

Microwave

Topo

(c) Tip-FMR MRFM with a coaxial resonator

Coaxial resonator

Conductive
magnetic layer

Topo

Figure 1. Schematic illustration of (a) the taping/lift mode MFM, (b) the tip-FMR MRFM with an external coaxial antenna, and (c) the tip-FMR MRFM with a coaxial resonator. In (b) and (c), the tip-sample distance is controlled with FM-AFM.

the stray magnetic field is strongly enhanced within 1 nm of the tip-sample distance, thereby improving the intensity of MFM signals. However, nonmagnetic forces, such as van der Waals forces and electrostatic forces derived from the local contact potential difference between the tip and the sample, are also enhanced, and these effects are inevitably superimposed on the MFM signals. In addition, as the tip oscillation amplitude is not controlled during the lift-scanning process, the tip may touch or withdraw from the sample surface because of thermal drift or strong local magnetic forces [6, 7]. Therefore, MFM imaging is unstable in the vicinity of the surface. For these reasons, the lift height is usually maintained within a few tens of nanometers, resulting in a reduction in spatial resolution.

To date, several techniques have been developed to extract magnetic force signals by this approach. These include subtraction of MFM signals obtained with a reverse-magnetized tip and a two-pass scanning method [8], bimodal tip oscillation to eliminate the short-range topographic force [9], and modulation of the magnetic force [10–13]. Among these approaches, the modulation method shows advantages in terms of force sensitivity. Usually the magnetic moment of a magnetically soft tip is oscillated by application of an alternating current (AC) magnetic field. However, to interpret the resulting MFM images, the magnetic states of the sample under an external field should be known. Furthermore, since the tapping/lift mode is used, MFM imaging in the vicinity of a surface is difficult.

Recently, an effective technique to extract the magnetic force by modulating ferromagnetic resonance (FMR) of a magnetic tip was proposed [14]. Since it utilizes the magnetic resonance, this technique is referred to as tip-FMR magnetic resonance force microscopy (tip-FMR MRFM). As depicted in figure 1(b), tip-FMR MRFM involves irradiating the ferromagnetic cantilever tip with evanescent microwaves through a coaxial open-ended antenna. By modulating the tip

magnetization induced by the irradiation of modulated microwave, the magnetic force is modulated and the modulation frequency component of the magnetic force is detected as an MRFM signal. This prevents perturbation of the magnetic state of the sample under an external field and improves separation of magnetic and nonmagnetic forces in the vicinity of surface. In tip-FMR MRFM, since the evanescent microwave field is spatially concentrated on the antenna surface, the antenna is carefully placed near to the tip at a distance of approximately 0.3 mm with a precise positioning device. Furthermore, the efficiency of tip-FMR excitation strongly depends on the tip-antenna angle and distance. Therefore, an alternative tip-FMR excitation method without the antenna makes the tip-FMR MRFM imaging method easier and more versatile.

In this study an alternative operation mode of tip-FMR MRFM is proposed. This technique is based on a coaxial resonator instead of the conventional external antenna as shown in figure 1(c). The main feature is the direct transmission of microwaves to the magnetic tip, achieved by electrically coupling the magnetic tip and the coaxial resonator. First, the theory of magnetic domain imaging using tip-FMR MRFM is introduced. Next, a design of the microwave transmission line is presented, and extraction of the tip-FMR frequency and excitation of the tip-FMR is verified. Finally, clear MRFM imaging of perpendicular nanometer-scale magnetic domain structures is demonstrated.

2. Theory

In tip-FMR MRFM, the hard magnetic cantilever tip, which is oscillated at a resonance frequency, f_0, using frequency modulation atomic force microscopy (FM-AFM), is irradiated by the modulated microwave. In the case of amplitude modulation of transmission microwave, the cantilever temperature periodically changes; this causes a fluctuation in f_0 which results in an unstable measurement. For this reason, a frequency-modulated microwave with constant power is used. The frequency-modulated microwave is described by the following equation:

$$f(t) = \cos\left\{2\pi f_{\text{rf}} t + \frac{f_{\text{d}}}{f_{\text{m}}} \sin\left(2\pi f_{\text{m}} t\right)\right\}. \tag{1}$$

Here, f_{rf}, f_{m}, and f_{d} are the carrier frequency, modulation frequency, and maximum frequency shift of f_{rf}, respectively. When f_{rf} coincides with the tip-FMR frequency, i.e., when the tip-FMR is excited, the tip magnetization, m, can be approximately described as follows [14]:

$$m(t) = m_{\text{dc}} + m_{\text{ac}} \cos(2\pi f_{\text{m}} t). \tag{2}$$

Here, m_{dc} is the direct current (DC) component, and m_{ac} is the AC component induced by the periodical change in the excitation ratio of tip-FMR. In the case of a hard magnetized tip, this approximation is thought to be valid unless the external field does not exceed the coecivity of the magnetic tip. We assume tip magnetization as a dipole magnetic
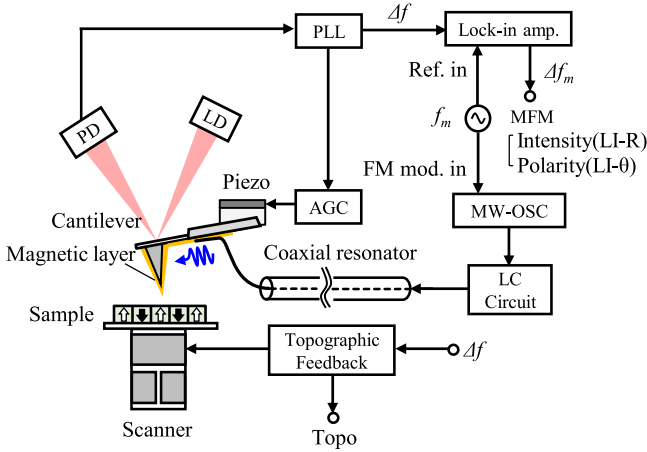
Figure 2. Block diagram of the tip-FMR MRFM with a coaxial resonator.

moment formed along the tip longitudinal direction [3]. This dipole approximation is suitable for a conventional magnetic tip fabricated without any sharpening techniques to make a high aspect ratio tip [15–17] which acts as a monopole. In FM-AFM, when the magnetic tip is oscillated perpendicularly to the sample surface and its oscillation amplitude is sufficiently smaller than the decay length of the conservative magnetic interaction forces, the induced frequency shift of the cantilever resonance Δf_{mag} is proportional to the force gradient [18] and thereby to the second derivative of perpendicular sample stray field, H_z, as follows:

$$\Delta f_{mag} = -\frac{f_0}{2k}\mu_0 m_z \frac{\partial^2 H_z}{\partial z^2}, \qquad (3)$$

where μ_0, k, z and m_z are vacuum permeability, the spring constant of the cantilever, the perpendicular tip-sample distance, and z component of m, respectively. From equations (2) and (3), the f_m component of Δf_{mag} (Δf_m) can be obtained as follows:

$$\Delta f_m = -\frac{f_0}{2k}\mu_0 m_{z(ac)}\frac{\partial^2 H_z}{\partial z^2}\cos(2\pi f_m t)$$
$$= -\frac{f_0}{2k}\mu_0 m_{z(ac)}\frac{\partial^2(-H_z)}{\partial z^2}\cos(2\pi f_m t \pm \pi). \qquad (4)$$

Here $m_{z(ac)}$ is the AC amplitude of m_z. This equation indicates that the amplitude of Δf_m is proportional to the $\partial^2 H_z/\partial z^2$. The reversal of the direction of H_z causes a phase shift of 180°, as shown in the second equation. Thus, by using AC modulation of the tip magnetic dipole moment induced by FMR, the surface magnetic domains and their polarity can be depicted simultaneously.

3. Experimental setup

Figure 2 depicts a block diagram of the tip-FMR MRFM with a coaxial resonator. FM-AFM mode is used to avoid the fluctuation effects of tip oscillation on the MRFM signal. The magnetic tip was oscillated at the resonance frequency, and the oscillation amplitude was kept constant with an FM-AFM controller (OC4, Specs Zurich GmbH) consisting of a phase

lock loop (PLL) and an automatic gain control circuit. The frequency shift, Δf, was detected by the PLL and used to adjust the tip-sample distance during the topographic scanning process in the FM-AFM mode. The microwave was generated by a microwave oscillator (MW-OSC) (MG3694B, Anritsu) and transmitted to the magnetic tip by impedance matching. The microwave frequency, f_{rf}, was set to the tip-FMR frequency and frequency-modulated at f_m. The f_m component of Δf (Δf_m) derived from the modulated magnetic force was detected by a lock-in amplifier using the modulation signal as a phase reference. The intensity and phase of Δf_m were recorded as magnetic intensity and polarity signals, respectively.

Figure 3 illustrates the microwave transmission line for feeding the microwave from the MW-OSC to the magnetic cantilever tip. It consists of a coaxial resonator and an LC circuit (L: inductor, C: capacitor), and works as an impedance matching. A flexible cable with inner and outer diameters of 0.5 and 1.0 mm, respectively, was used as a resonator. The cable length, ℓ, was set to $(1 + 2n)\lambda_{FMR}/4$ (λ_{FMR}: microwave wavelength at FMR frequency) to realize the resonance mode where the microwave reflection at the cable edge was minimized. Typically, a small value of n (1–3) was used for routing the cable and reducing transmission power loss. The edge of the cable core was connected to the cantilever base with silver paste. The LC circuit consisted of a series trimmer C and a parallel L. The circuit was surrounded by metal shield to protect it from the electromagnetic interference noise. The trimmer C was used to fine-tune the microwave transmission frequency.

A FePt-coated Si cantilever was used as an electrically conductive magnetic cantilever. FePt is a ferromagnetic material that can excite FMR without the application of an external magnetic field. In these materials, the energy levels of spins are split by an internal magnetic field according to the Zeeman Effect so that an FMR can occur due to microwave absorption without any external magnetic field [19]. The FePt-coated Si cantilever was fabricated as follows: first, a commercially available Si cantilever tip (PPP-NCLR, Nanosensors) was coated with a conductive ferromagnetic FePt film by radio-frequency sputter-coating. The FePt film covered the entire cantilever surface of the tip-side and the end part of cantilever base. The tip was then magnetized along the longitudinal direction under a pulsed magnetic field [20]. The cantilever was held on an insulator (PEEK plastic) support to reduce stray capacitance, which induces the shift of the matching frequency of the transmission lines.

All experiments were performed with a commercially available AFM instrument (JSPM-4210, JEOL Co.). The FMR frequency of the FePt tip was measured using electrical and force detection methods. In the electrical detection method, the dependence of the reflection coefficient, S_{11}, on the microwave frequency, f_{rf}, for the FePt tip was measured with a network analyzer (ENA E5071C, Agilent). For the force detection method, the dependence of the frequency shift, Δf, on f_{rf} for the FePt tip under a DC external field was measured using the FM-AFM setup. The DC magnetic field was applied by positioning the tip on an NdFeB permanent
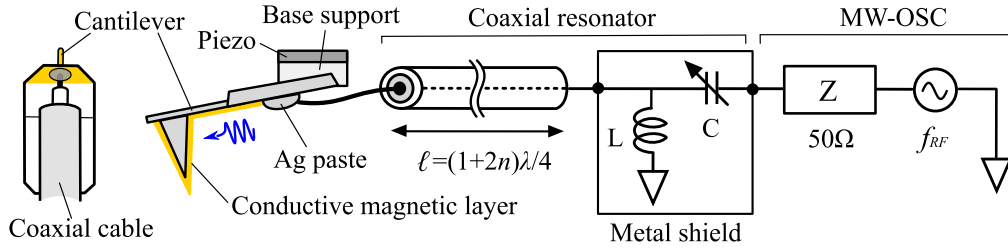
Figure 3. Schematic diagram of a microwave transmission line. The impedance was matched by adjusting the resonator length ℓ and the LC circuit. The left inset indicates the top view of the electrical connection between cantilever and coaxial cable core.
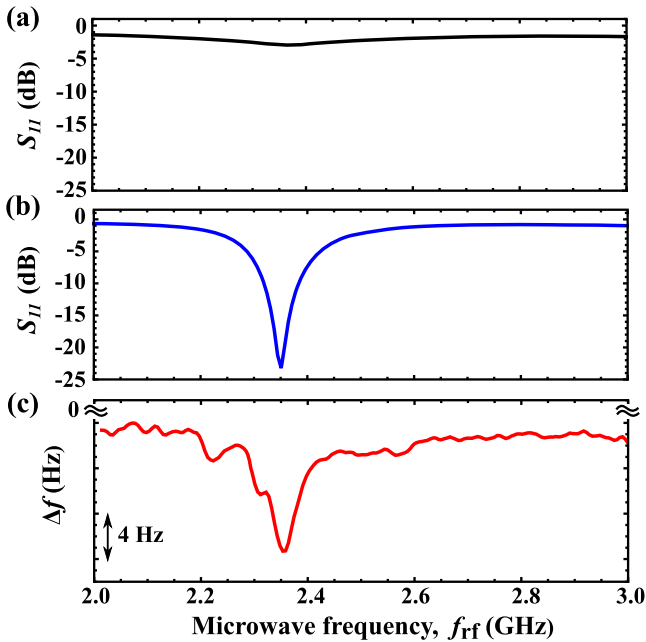
Figure 4. Microwave frequency f_{rf} dependence of the reflection coefficient S_{11} of a coaxial line (a) without z-matching and (b) with z-matching, respectively. The 30 nm thick FePt-coated Si cantilever was connected to the coaxial line. (c) f_{rf} dependence of Δf for the FePt-coated Si cantilever under a dc magnetic field obtained with the resonator. The cantilever oscillation parameters were the following: cantilever spring constant $k \approx 40 \, \mathrm{N \, m^{-1}}$, the first resonance frequency $f_0 = 255.6$ kHz, the quality factor $Q \approx 500$, and the oscillation amplitude $A = 20.0$ nm.

magnetic surface. The microwave power was set to be 20 dBm (100 mW), and the frequency was swept from 2.0 to 3.0 GHz. For the tip-FMR MRFM imaging, the microwave was frequency-modulated at $f_m = 500$ Hz with a deviation of 16 MHz. To effectively modulate the tip magnetization induced by excitation of FMR, the deviation was adjusted to be much lower than the full width of half maximum (FWHM) of the tip-FMR spectrum, typically ~50 MHz.

4. Results and discussion

Figure 4(a) depicts the f_{rf} dependence of the S_{11} (reflection spectrum) for the FePt tip connected to the resonator without z-matching. Here, a low value of S_{11} (dB) indicates a low reflection ratio and $S_{11} = 0$ dB indicates a reflection ratio of 1,

which means the microwave is fully reflected. As shown in figure 4(a), the spectrum features a small negative peak. The peak frequency is 2.358 GHz where S_{11} reached -3.0 dB slightly below the floor level, indicating the microwave adsorption induced by the FMR of the FePt film on the cantilever. Thus, the FMR frequency of the FePt film is 2.358 GHz. This value is well consistent with the FMR frequency of 2.367 GHz that was obtained by the antenna method [14] (not shown here). From this result, it can be concluded that extraction of the tip-FMR frequency is possible without the use of an external antenna.

Figure 4(b) depicts the f_{rf} dependence of S_{11} with z-matching. Z-matching was performed by using the resonator length $\ell \sim 9.6$ mm and the LC circuit tuned with $L \approx 1.5$ nH and $C \approx 3.0$ pF, providing a resonance adjusted to the tip-FMR frequency of 2.358 GHz (figure 4(a)). As depicted in figure 4(b), a single sharp notch peak with a FWHM of ~60 MHz is observed at 2.351 GHz. At this frequency, S_{11} reaches -23.23 dB, indicating a reduction of the reflection coefficient to 0.01, which means ~99.5% of the microwave power is transmitted to the resonator. Thus, the microwaves at tip-FMR frequency can be effectively transmitted to the cantilever by z-matching.

Excitation of the tip-FMR was confirmed by measuring the f_{rf} dependence of the frequency shift Δf (Δf (f_{rf}) curve) of the FePt tip. Figure 4(c) shows the Δf (f_{rf}) curve under an external DC magnetic field of ~230 mT for the same FePt tip used in the experiments shown in figures 4(a) and (b). Here, the decrease in Δf denotes an increase in the attractive forces acting on the tip. The floor level of Δf reflects the static magnetic force between the magnetic moment of the magnetized FePt tip and the applied external DC magnetic field, which has no f_{rf} dependence. The Δf (f_{rf}) curve has a large negative peak with a FWHM of ~50 MHz and some additional sub-peaks. The main peak depth of 9 Hz at 2.355 GHz coincides well with the electrically measured tip-FMR frequency. When the tip-FMR is excited, the DC magnetic moment increases, therefore, these peaks originate from additional attractive forces caused by excitation of the tip-FMR. The origin of sub-peaks at 2.23 and 2.30 GHz is thought to be multiple excitations of the FMR in FePt films formed on individual faces of pyramidal tip which FMR frequencies depend on the film morphologies [21, 22]. In addition, the excitation of the standing spin waves may be related [23]. Since at the outermost sub-peak frequency
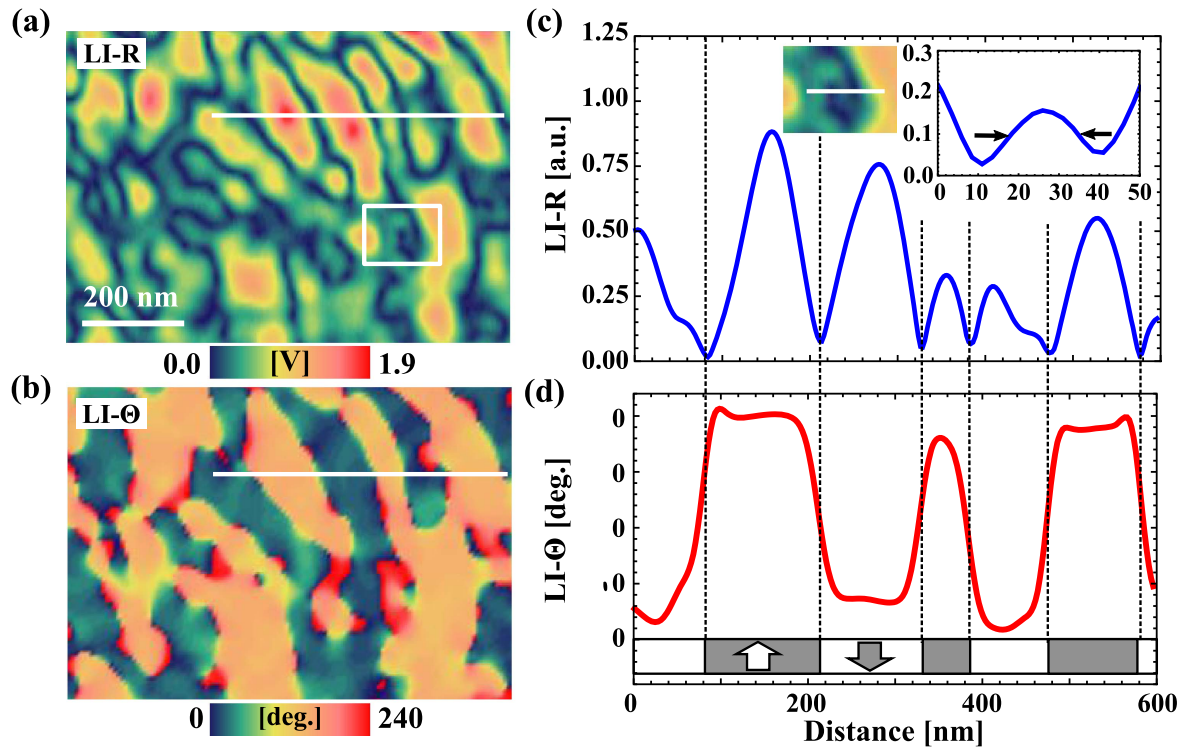
Figure 5. Tip-FMR MRFM images for (a) lock-in intensity (LI-R) and (b) phase (LI-θ) obtained on a 300 nm thick demagnetized FePt permanent magnet fabricated on a Si substrate. Line profiles taken along the white lines on (c) LI-R and (d) LI-θ images. The right inset in (c) indicates the LI-R profile along the white line in the left inset corresponding to the enlarged LI-R image of the white rectangular region in (a). The inset in (d) shows a cross-sectional view model of a demagnetized magnet consisting of alternating upward and downward magnetic domains represented by arrows. The scan size was 900×650 nm^2. The experimental parameters were as follows: cantilever spring constant $k \approx 40$ N m^{-1}, the first resonance frequency $f_0 = 295.9$ kHz, the quality factor $Q \approx 600$, and the oscillation amplitude $A = 5.0$ nm. The tip was scanned in constant height mode with tip-sample distance feedback off. The minimum tip-sample distance was within 1 nm on a highest protrusion.

(2.23 GHz), still $\sim$35% microwave is transmitted to the cantilever, taking into account of relatively high force sensitivity in FM-AFM, the appearance of these sub-peaks is plausible. These sub-peaks were also observed in previous work using coaxial antenna and their origins are discussed in detail [14]. Small oscillations such as noise come from the thermal effects induced by microwave transmission. It should be noted that the S_{11} curve with z-matching (figure 4(b)) does not exhibit these richer structures because the reflection reduction due to the z-matching is so high that any peaks induced by FMR microwave adsorption are masked. The typical minimum power necessary to excite the tip-FMR was about >5 dBm, which is lower than that for the antenna method. Thus, through the use of a coaxial resonator, it is possible to effectively excite a tip-FMR and detect it from a mechanical response of the tip oscillation.

MRFM imaging was performed on a demagnetized FePt thin-film perpendicular permanent magnet to demonstrate the effectiveness of tip-FMR MRFM with a resonator. Figures 5(a) and (b) depict lock-in magnitude (LI-R) and phase (LI-θ) images of Δf_{m}, respectively. The demagnetized state exhibits uniform up and down magnetic domain structures to minimize the magnetostatic energy on the whole surface [24]. Both the intensity and polarity images indicate a similar maze pattern contrast with a width of 10–100 nm, reflecting typical random magnetic domain structures of demagnetized states [25–27]. In

the intensity image, each domain appears as bright spots with dark boundaries, whereas the phase image shows domains as alternating regions of bright and dark contrast.

To identify the origins of the intensity and phase signals, figures 5(c) and (d) depict profiles measured along the white dotted lines in figures 5(a) and (b), respectively. The intensity peaks show an even symmetric profile, suggesting that perpendicular components are dominant in the tip magnetic moment [28] although small in-plane moment also contributes to MRFM signals because the tip oscillation is tilted slightly with respect to the sample surface. Therefore, these signals are thought to be derived from the strength modulation of perpendicular tip magnetization through the modulation of microwaves. The intensity reaches a maximum at the domain centers and becomes almost zero at the domain boundaries (indicated by vertical dotted lines). In contrast, the phase has binary values with a 180° phase difference that switches alternately at the boundaries. Therefore, the intensity and phase corresponded to the strength and the polarity (in the up and down directions) of the second derivative of the perpendicular stray field for each domain, respectively, as expressed in equation (4). These results indicate that the tip-FMR MRFM method can simultaneously image magnetic domains and their magnetic polarities. The right insets in figure 5(c) indicate that the LI-R profile obtained along the white line on the left inset image corresponding to the

zoomed-in LI-R image of a single domain indicated by the rectangular region in figure 5(a). The profile reveals the FWHM value as approximately 16 nm (indicated by arrow). This value is comparable to the lateral resolution for MFM using high aspect ratio magnetic tips fabricated by methods such as focus ion beam milling [15]. Thus, the excitation of tip-FMR using a coaxial resonator enables MRFM imaging with high spatial resolution.

5. Summary

An alternative operation mode of MRFM using the tip-FMR technique based on direct microwave transmission to a magnetic cantilever tip with a coaxial resonator was proposed. The utilization of a coaxial resonator with LC circuit enabled excitation of tip-FMR without an external antenna and tuning of the transmission frequency of microwave to the tip-FMR frequency. The tip-FMR frequency was electrically extracted from the S_{11} (f_{rf}) curve without z-matching using network analyzer. The measured tip-FMR frequency was confirmed by the excellent agreement of the peak frequencies between the S_{11} (f_{rf}) with z-matching and Δf (f_{rf}) curves obtained through the force detection method in FM-AFM. The capability of MRFM was successfully demonstrated by obtaining a clear up and down perpendicular magnetic domain contrast on a demagnetized permanent magnet film.

Acknowledgments

ORCID iDs

Yukinori Kinoshita ⬤ https://orcid.org/0000-0001-6248-0618

References

[1] Martin Y and Wickramasinghe H K 1987 *Appl. Phys. Lett.* **50** 1455

[2] Sáenz J J, García N, Grütter P, Meyer E, Heinzelmann H, Wiesendanger R, Rosenthaler L, Hidber H R and Güntherodt H-J 1987 *J. Appl. Phys.* **62** 4293

[3] Hartmann U 1999 *Annu. Rev. Mater. Sci.* **29** 53

[4] Zhong Q, Inniss D, Kjoller K and Elings V B 1993 *Surf. Sci.* **290** L688

[5] Abelmann L *et al* 1988 *J. Magn. Magn. Mater.* **190** 135

[6] Burnham N A and Colton R J 1989 *J. Vac. Sci. Technol.* A **7** 2906

[7] Yamaoka T, Tsujikawa H, Hirose R, Ito A, Kawamura H and Sakon T 2011 *J. Magn. Soc. Japan* **35** 60

[8] Cambel V, Precner M, Fedor J, Šoltýs J, Tóbik J, Ščepka T and Karapetrov G 2013 *Appl. Phys. Lett.* **102** 062405

[9] Li J W, Cleveland J P and Proksch R 2009 *Appl. Phys. Lett.* **94** 163118

[10] Proksch R, Skidmore G D, Dahlberg E D, Foss S, Schmidt J J, Merton C, Walsh B and Dugas M 1996 *Appl. Phys. Lett.* **69** 2599

[11] Proksch R, Neilson P, Austvold S and Schmidt J J 1999 *J. Appl. Phys. Lett.* **74** 1308

[12] Geng Y, Das H, Wysocki A L, Wang X, Cheong S-W, Mostovoy M, Fennie C J and Wu W 2014 *Nat. Mater.* **13** 163

[13] Saito H, Ito R, Egawa G, Li Z and Yoshimura S 2011 *J. Appl. Phys.* **109** 07E330

[14] Arima E, Naitoh Y, Li Y J, Yoshimura S, Saito H, Nomura H, Nakatani R and Sugawara Y 2015 *Nanotechnology* **26** 125701

[15] Phillips G N, Siekman M, Abelmann L and Lodder J C 2002 *Appl. Phys. Lett.* **81** 865

[16] Wu Y, Shen Y, Liu Z, Li K and Qiu J 2003 *Appl. Phys. Lett.* **82** 1748

[17] Winkler A, Mühl T, Menzel S, Kozhuharova-Koseva R, Hampel S, Leonhardt A and Büchner B 2006 *J. Appl. Phys.* **99** 104905

[18] Albrecht T R, Grütter P, Horne D and Rugar D 1991 *J. Appl. Phys.* **69** 668

[19] Kittel C 2004 *Introduction to Solid State Physics* 8th edn (New York: Wiley) 379

[20] Zheng Y, Yoshimura S, Egawa G, Zheng F, Kinoshita Y and Saito H 2015 *J. Appl. Phys.* D **48** 335006

[21] Hurben M J and Patton C E 1998 *J. Appl. Phys.* **83** 4344

[22] Butera A, Zhou J N and Barnard J A 1999 *Phys. Rev.* B **60** 12270

[23] Martins A, Trippe S C, Santos A D and Pelegrini F 2007 *J. Magn. Magn. Mater.* **308** 120

[24] Chikazumi S 1984 *Physics of Ferromagnetism* vol 2 (Tokyo: Shokabo) 196

[25] Szmaja W, Grobelny J, Cichomski M, Makita K and Rodewald W 2004 *Phys. Status Solidi* a **201** 550

[26] Schwarz A and Wiesendanger R 2008 *Nano Today* **3** 28

[27] Thielsch J, Stopfel H, Wolff U, Neu V, Woodcock T G, Güth K, Schultz L and Gutfleisch O 2012 *J. Appl. Phys.* **111** 103901

[28] Mamin H J, Rugar D, Stern J E, Terris B D and Lambert S E 1988 *Appl. Phys. Lett.* **53** 1563